

Burkholderia pseudomallei Isocitrate Lyase Is a Persistence Factor in Pulmonary Melioidosis: Implications for the Development of Isocitrate Lyase Inhibitors as Novel Antimicrobials^{∇†}

Erin J. van Schaik, Marina Tom, and Donald E. Woods*

Department of Microbiology and Infectious Diseases, Faculty of Medicine, University of Calgary Health Science Centre, 3330 Hospital Drive NW, Calgary, Alberta T2T 4N1, Canada

Received 29 May 2009/Accepted 10 July 2009

Burkholderia pseudomallei, the causative agent of melioidosis, has often been called the great “mimicker,” and clinical disease due to this organism may include acute, chronic, and latent pulmonary infections. Interestingly, chronic pulmonary melioidosis is often mistaken for tuberculosis, and this can have significant consequences, as the treatments for these two infections are radically different. The recurrent misdiagnosis of melioidosis for tuberculosis has caused many to speculate that these two bacterial pathogens use similar pathways to produce latent infections. Here we show that isocitrate lyase is a persistence factor for *B. pseudomallei*, and inhibiting the activity of this enzyme during experimental chronic *B. pseudomallei* lung infection forces the infection into an acute state, which can then be treated with antibiotics. We found that if antibiotics are not provided in combination with isocitrate lyase inhibitors, the resulting *B. pseudomallei* infection overwhelms the host, resulting in death. These results suggest that the inhibition of isocitrate lyase activity does not necessarily attenuate virulence as previously observed for *Mycobacterium tuberculosis* infections but does force the bacteria into a replicating state where antibiotics are effective. Therefore, isocitrate lyase inhibitors could be developed for chronic *B. pseudomallei* infections but only for use in combination with effective antibiotics.

Burkholderia pseudomallei is a gram-negative soil bacterium that causes the disease melioidosis (5). Melioidosis was originally recognized and is known to be endemic to Southeast Asia and Northern Australia; however, cases have been reported for other areas in the southern hemisphere (4). Presentations of *B. pseudomallei* infections can result in an asymptomatic state, benign pneumonitis, acute pneumonia, chronic pneumonia, or overwhelming septicemia (39). As the clinical manifestations are vast and varied, infections due to *B. pseudomallei* are often misdiagnosed (13). The most common misdiagnosis for pulmonary *B. pseudomallei* infections is tuberculosis (25, 37). This misdiagnosis has serious repercussions, as the treatments for *B. pseudomallei* and *Mycobacterium tuberculosis* infections are very different (10, 26). In addition to these clinical similarities, we have described significant similarities between the pathological changes associated with tuberculosis and those seen in a chronic melioidosis animal model that we have developed, which include multiple-granuloma formation (36). Besides the similar lung pathology, both *B. pseudomallei* and *M. tuberculosis* infections can enter into a dormant phase, where there are no signs of infection (8, 24).

Latency is a well-defined stage during *M. tuberculosis* infections, and a number of recent studies have described factors involved in the establishment of a latent infection (29). Little is

known about latent *B. pseudomallei* infections, but the striking similarity to *M. tuberculosis* infections has led to speculations that these organisms use similar pathways to produce latency (8). For example, both *M. tuberculosis* and *B. pseudomallei* are able to survive for long periods of time in a dormant or non-dividing state in vitro (20, 38), and it has been hypothesized that these organisms may remain in a similar state during latent pulmonary infections. Both *B. pseudomallei* and *M. tuberculosis* are intracellular pathogens and clearly have metabolic systems enabling survival in this environment. Very little is known about the in vivo metabolism within phagocytic cells; however, the likely major carbon source during chronic *M. tuberculosis* lung infections is fatty acids, which can be metabolized by the glyoxylate shunt and the β -oxidation cycles (17, 21, 22). It was previously determined that *M. tuberculosis* requires isocitrate lyase (ICL) from the glyoxylate shunt, an enzyme involved in the metabolism of fatty acids for the production of a persistent infection (17, 21). *M. tuberculosis* produces two distinct ICL enzymes, ICL-1 and ICL-2, that are jointly required for growth in vivo (21). Having demonstrated that *B. pseudomallei* is an intracellular pathogen that causes lung pathology similar to that caused by tuberculosis (36), we wished to determine if fatty acid metabolism is required for persistent *B. pseudomallei* infections.

MATERIALS AND METHODS

Bacterial strains and plasmids. The parental *Burkholderia pseudomallei* strains used in this study were 1026b, a clinical isolate, and DD503, a derivative of 1026b ($\Delta amrR$ - $oprA$) *rpsL* (18). *Escherichia coli* TOP10 (Invitrogen) and *E. coli* SM17 λ pir (6) cells were routinely used for transforming cloned plasmids and mating procedures, respectively. Bacterial cells were grown in Luria-Bertani (LB) broth at 37°C for all procedures unless otherwise indicated. The following plasmids were utilized in this study: pCR2.1-TOPO (Invitrogen), pBluescript SKII (Stratagene), pKAS46 (30), pTNS2, and pUC18Tmini-Tn7-Gm (3).

* Corresponding author. Mailing address: Department of Microbiology and Infectious Diseases, Faculty of Medicine, University of Calgary Health Sciences Centre, 3330 Hospital Drive NW, Calgary, Alberta T2N 4N1, Canada. Phone: (403) 220-2564. Fax: (403) 210-8504. E-mail: woods@ucalgary.ca.

† Supplemental material for this article may be found at <http://iai.asm.org/>.

[∇] Published ahead of print on 20 July 2009.

Mutant strain construction. *B. pseudomallei* deletion mutants were constructed using a previously described allelic exchange protocol (27). The genes for this study were selected using the metabolic pathway information in the KEGG database for the K96243 annotated genome (<http://www.genome.jp/kegg/>) (15). The primers were then designed using the K96243 annotated genome sequences. Genes were PCR amplified from 1026b genomic DNA using a HotStarTaq master mix kit (Qiagen). In-frame deletions of approximately 600 bp were created by PCR cloning and ligation of up- and downstream fragments or SOEing PCR (11) (see the supplemental material). All of the deletion mutants were sequenced, and their sequences were compared directly to the K96243 genome sequence. All mutant sequences were identical to the K96243 genome sequences for the selected annotated genes. The in-frame stitched deletion fragments were then cloned into pKAS46 using the 5' KpnI and 3' XbaI sites and transformed into *E. coli* SM17 λ pir cells. The pKAS46 plasmid containing the desired deletion fragment was then mated into *B. pseudomallei* DD503 cells and selected first on LB broth containing 100 μ g/ml polymyxin B (Sigma) and 25 μ g/ml kanamycin (Sigma), followed by selection on LB broth containing 250 μ g/ml streptomycin (Sigma). Allelic exchange of the deletion fragment was confirmed using PCR. Primer sequences are listed in the supplemental material. The pGSV3-*lux* ICL mutant was constructed using a 500-bp internal fragment of the ICL gene using a previously described protocol (19).

Complementation studies. The *B. pseudomallei* in-frame deletion mutants were complemented using the mini-Tn7 system (3). The genes were PCR amplified from 1026b genomic DNA with 200 bp upstream and downstream of the start and stop codons, respectively, and contained KpnI sites on both the 5' and 3' ends. The resulting fragments were digested with KpnI, ligated into plasmid pUC18T mini-Tn7-Gm, and transformed into *E. coli* TOP10 cells. The resulting plasmids were purified using a QIAprep Spin miniprep kit (Qiagen) and electroporated into the DD503 mutant strain with helper plasmid pTNS2. Transformants were selected on LB broth containing 50 μ g/ml gentamicin, and positive clones were confirmed using PCR primers for the three *glmS* genes and the mini-Tn7 within the *B. pseudomallei* genome. All of the complement fragments were inserted within the *attTn7* site downstream of the BPSL1312 *glmS* gene (data not shown). Primer sequences are listed in the supplemental material.

Rat infections. Male Sprague-Dawley rats (200 to 220 g) were infected with *B. pseudomallei* strains either in phosphate-buffered saline (PBS) or encased in agar beads via the intratracheal route as previously described (36).

Acute infections. Six rats per group were inoculated intratracheally with one of four different doses made in PBS (10^2 , 10^3 , 10^4 , and 10^5 cells) of each *B. pseudomallei* parental, mutant, or complemented strain as previously described (36). Animals were monitored carefully for three consecutive days for signs of morbidity and mortality. Fifty percent lethal doses were calculated according to a method described previously by Reed and Muench (28).

Chronic infections. Four groups of eight rats per group were used for the chronic infection experiments. All animals in each group were inoculated intratracheally with 10^3 *B. pseudomallei* strain 1026b cells encased in agar beads as previously described (36). The rats in one group remained untreated. At day 7, 100 μ l of itaconic acid solution in normal saline (0.9% [vol/vol] NaCl) was administered intranasally (50 μ l per nostril) to all animals in two of the groups. This intranasal treatment was repeated 2 days later, at which point all of the rats in one of these itaconic acid-treated groups and all of the rats in one of the untreated groups were treated with 100 μ l of 300 μ g/ml ceftazidime via intraperitoneal injection. Two days after the ceftazidime treatment, the lungs from five surviving animals in each group were removed aseptically and homogenized in 3 ml PBS followed by serial dilution and plating onto LB agar. Statistical analysis (analysis of variance) of differences in quantitative bacteriology between groups was performed using GraphPad Prism, version 5.00, for Windows (GraphPad Software). In addition, the lungs of three surviving animals from each group were removed and fixed using 10% formalin, followed by staining with hematoxylin and eosin. Mounted lung sections were examined by light microscopy for qualitative pathological changes using an Olympus IX70 microscope, and images were taken using a cooled 12-bit charge-coupled-device Retiga EXi camera (QImaging). Image analysis was performed using Volocity 4.2.0 software (Improvision Ltd.).

Metabolic analysis. *B. pseudomallei* parental and mutant strains were grown overnight at 37°C on BUG agar (Biolog). The bacteria were swabbed from the surface of the BUG agar plates and resuspended in GN/GP inoculating fluid (Biolog) to reach a density of ~50% turbidity. The bacterial suspensions were then added to each well of the GN2 microplate at a volume of 150 μ l and incubated overnight at 37°C. GN2 microplate assays were performed in duplicate, and the results were inspected visually and at an optical density of 600 nm. In addition, the *B. pseudomallei* parental and mutant strains were grown overnight in LB broth and then washed twice with M9 minimal medium without a carbon source. The bacteria were then resuspended in M9 minimal medium

without a carbon source and inoculated into a microplate with wells containing M9 minimal medium plus 0.2% glucose, 0.2% glycerol, 0.2% citrate, 0.2% acetate, or 0.2% propionate and incubated overnight at 37°C. The carbon source microplate assays were performed in duplicate, and the results were read at an optical density of 600 nm. In addition, *lux*-mediated light production was monitored after 24 and 48 h of growth using 200- μ l aliquots of culture in a System-Sure luminometer (Nova Biomedical).

Enzyme assays. Both the mutant and parental strains were grown overnight at 37°C in 25 ml LB broth supplemented with 1% acetate. The cells were harvested, resuspended in 4 ml Tris-EDTA buffer, and sonicated. ICL enzyme assays were performed according to Sigma protocol EC 4.1.3.1 using 100 μ l of cell lysate. The aconitase (ACN) enzyme assays were performed according to Sigma protocol EC 4.2.1.3 using 50 μ l of cell lysate. The quantity of protein in the cell lysates was determined using a BCA assay (Pierce). These enzyme assays were performed in triplicate, and Student *t* test statistical analysis was performed using GraphPad Prism, version 5.00, for Windows (GraphPad Software).

Macrophage infections. RAW 264.7 murine macrophage cells were maintained in Dulbecco's modified Eagle's medium (Invitrogen) supplemented with 10% (vol/vol) fetal bovine serum (Invitrogen), 100 μ g/ml penicillin, 100 μ g/ml streptomycin, and 250 μ g/ml amphotericin B at 37°C under 5% CO₂. The cells were seeded into 24-well tissue culture plates at a density of $\sim 1 \times 10^6$ cells/ml and incubated overnight for the macrophage infection assays. The *B. pseudomallei* parental and mutant strains were grown overnight at 37°C, washed three times with PBS, and resuspended in Dulbecco's modified Eagle's medium to a multiplicity of infection of 10. The macrophage infection assays were performed using a modified kanamycin protection assay, which was described previously (2). At 3, 6, 12, and 24 h after infection, the culture supernatant was removed to perform cytotoxicity assays for lactate dehydrogenase using a CytoTox 96 non-radioactive kit (Promega). In addition, the monolayers were lysed with 0.25% (vol/vol) Triton X-100, and serial dilutions were plated onto LB agar. These macrophage infection assays were performed in triplicate, and Student *t* test statistical analysis against the DD503 parental strain was performed using GraphPad Prism, version 5.00, for Windows (GraphPad Software).

RESULTS

Metabolic and enzymatic potential of *B. pseudomallei* strains.

In-frame deletion mutations were created to inactivate genes coding for a number of enzymes from the tricarboxylic acid (TCA) cycle, the glyoxylate shunt, and the methyl-citrate pathways (Fig. 1A). The TCA cycle completes the oxidation of acetyl coenzyme A (CoA) produced by the metabolism of both glucose and fatty acids (23). The glyoxylate shunt is used to replenish TCA cycle intermediates during growth on fatty acids (22). Finally, the methyl-citrate pathway was used to further oxidize propionyl-CoA produced by the β -oxidation of odd-chain fatty acids (23). The genetic organization of the methyl-citrate pathway is displayed in Fig. 1C.

The strains were grown in LB broth at 37°C to determine if there were any differences during *in vitro* growth. There were no significant differences between the *in vitro* growth rates of the parental and mutant strains in rich medium (Fig. 1B). Although there were no significant differences in growth rates *in vitro*, there was a slight surge in growth at 2 h for the Δ BPSS0209 mutant (PrpF) (Fig. 1B). Therefore, the ability of these organisms to grow on several carbon sources was tested to determine their metabolic potentials. Interestingly, all of the mutants were able to grow in M9 medium supplemented with glucose, glycerol, acetate, citrate, or propionate (data not shown). This was unexpected, as previous reports have shown that the inactivation of either the ACN or ICL enzyme in other pathogenic bacteria prevents growth on acetate as the sole carbon source (7, 17, 32). *B. pseudomallei* possesses an additional aconitase gene, BPSS1726, the product of which may account for the ability of the ACN mutant to grow on acetate. The ability of the 2-methylisocitrate lyase (MCL) and the ICL/

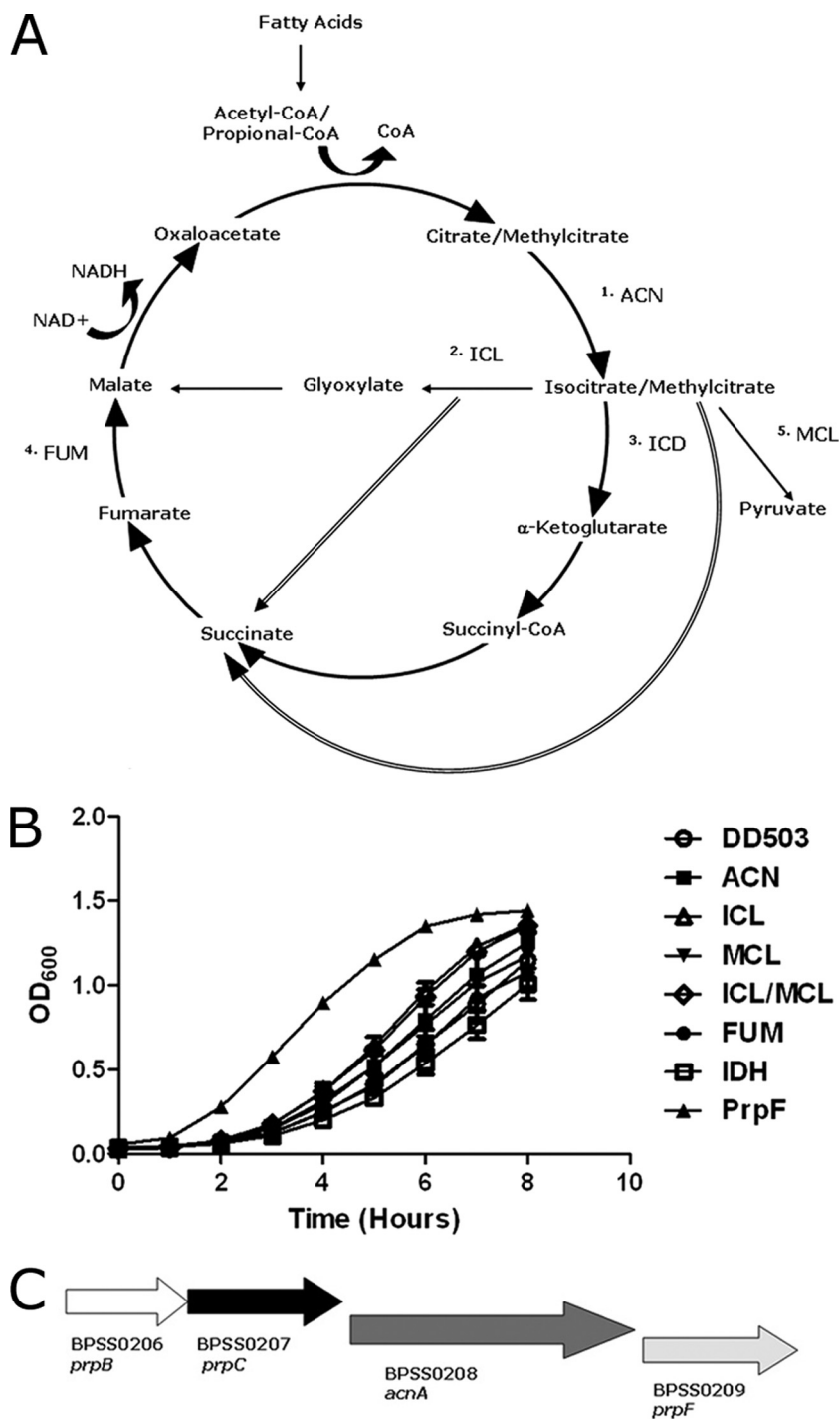


FIG. 1. Glyoxylate shunt, TCA, and β-oxidation pathway mutants. (A) β-Oxidation of fatty acids produces either acetyl-CoA or propionyl-CoA, which can be further metabolized by the glyoxylate and methylcitrate cycles, respectively. 1, ACN (ΔBPSS0208); 2, ICL (ΔBPSSL2188); 3, isocitrate dehydrogenase (ICD) (ΔBPSS0011, homologue to BPSL0896); 4, fumarate hydratase (FUM) (ΔBPSSL2469); 5, MCL (ΔBPSS0206). These genes were selected using the KEGG metabolic pathways for *B. pseudomallei* strain K96243. (B) In vitro growth characteristics of the mutants used in this study (*n* = 3; error bars represent means ± standard errors of the means [SEM]). *B. pseudomallei* strains were inoculated into LB broth and monitored for growth using the optical density at 600 nm (OD₆₀₀). (C) Genomic organization of the methylcitrate operon, which is present on chromosome II of the *B. pseudomallei* genome.

MCL mutants to grow on propionate was not unexpected, as it was previously shown that the inactivation of these enzymes does not prevent the ability of *Mycobacterium smegmatis* to grow on propionate as the sole carbon source (35).

We also examined the metabolic fingerprints of parental and mutant *B. pseudomallei* strains using GN2 plates (Biolog), and although there were notable differences between the parental and mutant strains, no differences in acetate

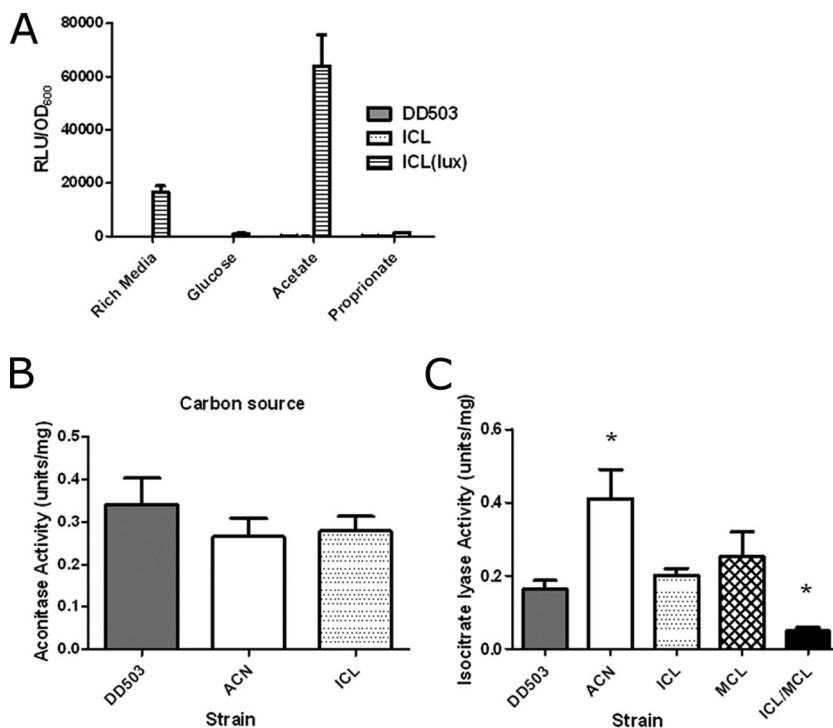


FIG. 2. ACL and ICL enzymatic activities of *B. pseudomallei* parental and mutant strains. (A) ICL expression was monitored using relative light production after growth in LB broth or M9 medium plus 0.2% glucose for 24 h and M9 medium plus 0.2% acetate or M9 medium plus 0.2% propionate after 48 h. RLU stands for relative light units (luminescence). OD₆₀₀, optical density at 600 nm. (B) ACN activity (1 unit catalyzes the formation of 1 μ mol of citrate to isocitrate per minute; $n = 3$; error bars represent means \pm SEM). Cell extracts were collected after sonication of *B. pseudomallei* cultures grown overnight in LB broth plus 1% acetate. (C) ICL activity (1 unit catalyzes the formation of 1 μ mol of glyoxylate per minute; $n = 3$; error bars represent means \pm SEM). *, significantly different ($P < 0.05$) from DD503 using paired Student *t* tests.

metabolism were observed (see the supplemental material). The gene expression levels of ICL were examined under different growth conditions using luciferase activity in a pGSV-*lux* ICL mutant, which results in luciferase production under the control of the ICL promoter. The activity of the ICL promoter was significantly upregulated during growth on acetate, indicating that ICL is involved in acetate metabolism even if there is another system in place to metabolize acetate in the absence of ICL (Fig. 2A).

Enzymatic assays were performed to determine whether or not the parental or mutant strains had differences in ACN and/or ICL activity. There was no difference in the ACN activities between parental strain DD503 and the ACN and ICL mutant strains (Fig. 2B), which is likely due to the second ACL gene product, which may be able to compensate for the *acnA* deletion. There was no difference in the ICL activity of parental strain DD503 and the single ICL and MCL mutant strains (Fig. 2C); however, when both the ICL and MCL genes were inactivated, there was a significant decrease in the level of ICL activity (Fig. 2C). This suggests that MCL has ICL activity and can substitute for the ICL enzyme, which is not surprising considering that ICL-1 from *M. tuberculosis* functions as both an ICL and an MCL (9). Interestingly, the ACN mutant strain had a significant increase in ICL activity (Fig. 2C). Having characterized their enzymatic activities, we determined the ability of the mutants to establish acute and chronic infection.

ICL is required for production of chronic *B. pseudomallei* infection and also has an effect during acute infections. The *B. pseudomallei* ICL mutant was unable to establish a chronic infection (35), similar to results obtained with *M. tuberculosis* (17, 21) (Table 1). The mutation of ICL-1 from *M. tuberculosis* resulted in an inability to establish a chronic infection due to a reduction in virulence (17). In contrast, the *B. pseudomallei* ICL mutant was hypervirulent. It did not establish a chronic infection but established an acute infection, as demonstrated by an increase in the mortality rate and the number of bacteria recovered from the lungs compared to the parental strain (Table 1). The ability of the ACN mutant to establish a chronic infection was also tested, since ACN activity has been linked to virulence in several bacterial species (31, 32). Interestingly, the ACN mutant was able to establish a chronic infection even at bacterial inocula that would cause lethality with the parental DD503 strain, and similar numbers of bacteria were recovered from the lungs regardless of the infectious dose (Table 1).

The ability of the deletion mutants to cause an acute infection was also tested (Table 2). The ICL mutant was also hypervirulent during an acute infection. This differs from *M. tuberculosis* since an ICL-1 mutation had no effect on the acute stage of infection (17). Furthermore, when both of the ICL genes were mutated in *M. tuberculosis*, these mutants were no longer capable of growth in vivo (21). A mutation of MCL in *B. pseudomallei* resulted in a minor decrease in virulence; how-

TABLE 1. Influence of ICL and ACN mutations on chronic *Burkholderia pseudomallei* rat lung infections

Strain (inoculum size)	No. of survivors/total no. of rats	Mean CFU (range) ^a	
		Day 7	Day 14
DD503 (10 ⁵)	0/6	ND	ND
DD503 (10 ⁴)	0/6	ND	ND
DD503 (10 ³)	4/6	1.3 × 10 ⁴ (3.7 × 10 ³ –4.3 × 10 ⁴)	4.1 × 10 ⁴ (1.6 × 10 ⁴ –6.3 × 10 ⁴)
DD502 (10 ²)	6/6	3.8 × 10 ⁴ (8.9 × 10 ³ –7.0 × 10 ⁴)	7.7 × 10 ³ (1.5 × 10 ³ –1.1 × 10 ⁴)
ICL (10 ⁵)	0/6	ND	ND
ICL (10 ⁴)	0/6	ND	ND
ICL (10 ³)	2/6	6.7 × 10 ⁵ (3.5 × 10 ⁵ –8.1 × 10 ⁵)	7.3 × 10 ⁵ (4.1 × 10 ⁵ –9.0 × 10 ⁵)
ICL (10 ²)	4/6	4.1 × 10 ⁶ (2.2 × 10 ⁶ –9.1 × 10 ⁶)	1.9 × 10 ⁶ (5.9 × 10 ⁵ –4.4 × 10 ⁶)
ACN (10 ⁵)	6/6	4.6 × 10 ⁵ (2.0 × 10 ⁵ –6.3 × 10 ⁵)	2.3 × 10 ⁵ (9.6 × 10 ⁴ –5.5 × 10 ⁵)
ACN (10 ⁴)	6/6	3.9 × 10 ⁵ (1.4 × 10 ⁵ –6.7 × 10 ⁵)	2.0 × 10 ⁵ (8.7 × 10 ⁴ –5.5 × 10 ⁵)
ACN (10 ³)	6/6	5.1 × 10 ⁵ (2.4 × 10 ⁵ –7.3 × 10 ⁵)	6.2 × 10 ⁵ (2.9 × 10 ⁵ –8.1 × 10 ⁵)
ACN (10 ²)	6/6	6.3 × 10 ⁵ (3.0 × 10 ⁵ –8.7 × 10 ⁵)	5.9 × 10 ⁵ (3.3 × 10 ⁵ –9.1 × 10 ⁵)

^a ND, not done.

ever, the mutation of both MCL and ICL resulted in a radical increase in virulence (Table 2). Complementation of the mutant strains restored the wild-type phenotype except for ACN, where we were unable to create a complemented strain. The *acnA* gene is found in an operon with the MCL (*prpB*), *prpC*, and BPSS0209 (*prpF*) genes (Fig. 1C). Therefore, we created a deletion in BPSS0209 to show that the ACN mutant phenotype was not due to a polar defect in this gene. The ΔBPSS0209 mutant was hypervirulent in the acute infection model, indicating that the phenotype of the ACN mutant was not due to a polar effect (Table 2). Although the mutation of the *acnA* gene caused a reduction in the level of virulence of *B. pseudomallei*, mutations of several other genes from the TCA cycle (fumarate hydratase and isocitrate dehydrogenase) had little or no effect on the course of an acute infection (Fig. 1A and Table 2).

ICL is not required for survival within unactivated macrophage cells; however, ICL mutants are significantly more cytotoxic than other *B. pseudomallei* strains. All of the strains with deletion mutations that altered virulence during the course of chronic or acute lung infections except ΔBPSS0209 were tested for their ability to survive within mouse RAW 264.7 macrophage cells. All of the strains were taken up by the macrophage cells at comparable levels, as indicated by the

number of intracellular bacteria at the 3-h time point (Fig. 3A). The replication of the parental DD503 strain peaked at 6 h, whereas the replication of the hypervirulent ICL and ICL/MCL mutants peaked at 12 h (Fig. 3A). The cytotoxicity of the parental and mutant strains for macrophage cells was also evaluated using lactate dehydrogenase release as a measure of cellular viability and integrity. The hypervirulent ICL and ICL/MCL strains were significantly more cytotoxic at the 3-, 6-, and 12-h time points (Fig. 3B, C, and D, respectively). The increased macrophage cytotoxicity correlates well with the significant increase in virulence observed with the acute infection model (Table 2). In addition, the reduced cytotoxicity of the ACN strain correlates well with this strain's increased ICL activity (Fig. 2B) and decreased virulence (Table 2). However, there was no significant difference between the cytotoxicities of the parental and mutant strains at 24 h (data not shown). This suggests that these strains may actively kill the macrophage cells due to a defective production of the glyoxylate shunt enzyme ICL. Consequently, we hypothesize that the inhibition of the enzymatic function of ICL forces *B. pseudomallei* out of the macrophage and onto an acute infectious path.

Inhibition of ICL enzymatic activity during chronic *B. pseudomallei* infection forces the infection into an acute phase. To test this hypothesis, the ability of itaconic acid, a previously established potent competitive inhibitor of ICL, to inhibit the ICL activity of clinical strain 1026b was determined (Fig. 4A) (12). The addition of 1 mg/ml itaconic acid to the 1026b ICL enzyme assay reduces the activity to 42% of the uninhibited control (Fig. 4A). Therefore, itaconic acid is a potent inhibitor of the ICL activity from *B. pseudomallei* clinical strain 1026b. Chronic *B. pseudomallei* lung infections were established in rats using clinical strain 1026b. The establishment of a chronic infection was confirmed by microscopic visualization of lung pathology after 7 days of infection (Fig. 4B). Lung histopathology clearly shows the formation of granulomas, which is similar to previously reported lung histopathology obtained for chronic *B. pseudomallei* lung infection (36). At 7 days postinfection, the rats were treated intranasally with itaconic acid; this treatment was repeated 2 days later with or without a concomitant intraperitoneal treatment with ceftazidime. Chronically infected rats that were treated with itaconic acid had high bacterial loads within the lungs, indicating that the bacteria were actively

TABLE 2. Lethality of parental, mutant, and mutant complemented *B. pseudomallei* strains during acute rat lung infections

Strain ^a	LD ₅₀ ^b
DD503.....	4.6 × 10 ⁴
ACN.....	>10 ⁵
ACN complement.....	ND
ICL.....	2.1 × 10 ³
ICL complement.....	5.5 × 10 ⁴
FUM.....	1.1 × 10 ⁴
FUM complement.....	4.6 × 10 ⁴
ICD.....	3.9 × 10 ⁴
ICD complement.....	4.0 × 10 ⁴
MCL.....	9.2 × 10 ⁴
MCL complement.....	3.8 × 10 ⁴
ICL/MCL.....	<10 ³
ΔBPSS0209.....	<10 ³

^a For strain descriptions, see the legend of Fig. 1A.

^b LD₅₀, 50% lethal dose calculated according to the method described previously by Reed and Muench (28). ND, not done.

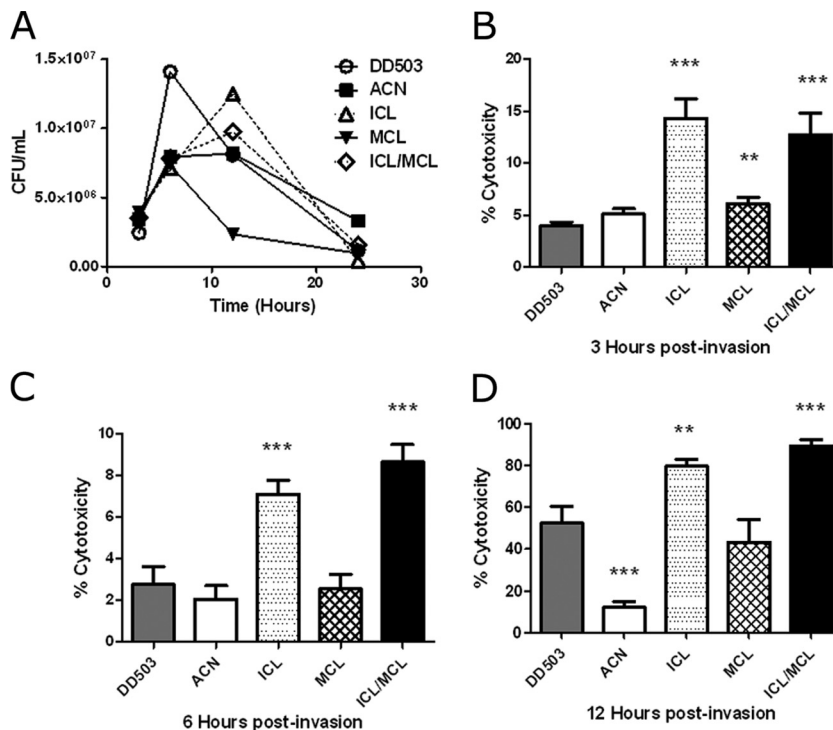


FIG. 3. Survival and cytotoxicity of *B. pseudomallei* parental and mutant strains in RAW 264.7 macrophage cells. (A) RAW 264.7 macrophage cells were infected at a multiplicity of infection of 10 and allowed to invade for 1 h, and the number of intracellular bacteria was then determined at 3, 6, 12, and 24 h postinfection. The means \pm SEM of data from at least three independent experiments are shown. (B to D) Cytotoxicities of the *B. pseudomallei* strains were measured using lactate dehydrogenase release at 3, 6, and 12 h, respectively. The means \pm SEM of data from at least three independent experiments are shown. *, significantly different ($P < 0.05$) from DD503 using paired Student *t* tests.

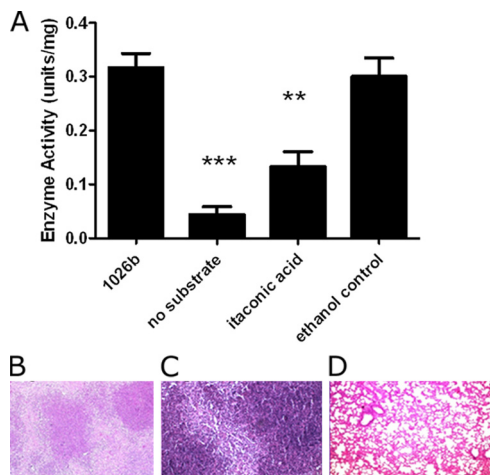


FIG. 4. Effects of itaconic acid on chronic *B. pseudomallei* lung infection. (A) Cell extracts were collected after sonication of 1026b cultures grown overnight in LB broth plus 1% acetate. Shown are data for ICL activity (1 unit catalyzes the formation of 1 μ mol of glyoxylate per minute in the presence of 1 mg/ml itaconic acid; $n = 3$; error bars represent means \pm SEM). *, significantly different ($P < 0.05$) from 1026b using paired Student *t* tests. (B) Microscopic examination (hematoxylin and eosin stained; magnification, $\times 100$) of rat lung chronically infected with *B. pseudomallei* strain 1026b at 7 days postinfection. (C) Microscopic examination (hematoxylin and eosin stained; magnification, $\times 100$) of chronically infected rat lung after intranasal treatment with itaconic acid. (D) Microscopic examination of uninfected rat lung after treatment with itaconic acid (magnification, $\times 100$).

dividing (log mean bacterial load \pm standard deviation of 6.2 ± 0.25 for treatment with itaconic acid only [with a P value of <0.001 indicating a significant difference from values for the no-treatment group]). This was not seen in rats that received no treatment, where the bacterial loads remained constant throughout the infection (log mean bacterial load \pm standard deviation of 4.6 ± 0.07 for no treatment), as previously demonstrated (36). The lung pathology noted for rats treated with itaconic acid versus no treatment further supports the hypothesis that itaconic acid converts a chronic/latent *B. pseudomallei* lung infection into an acute infection (Fig. 4C). The lung histopathology clearly shows the mass infiltration of immune cells, which is similar to previous lung histopathology obtained for acute *B. pseudomallei* lung infection (36). Itaconic acid had no effect on the lung pathology of uninfected control rats (Fig. 4C). The most remarkable finding was that treatment of rats with itaconic acid followed by treatment with ceftazidime reduced the bacterial load more so than did treatment with ceftazidime alone (log mean bacterial loads \pm standard deviations of 4.7 ± 0.07 for treatment with ceftazidime only [with a P value of <0.001 indicating a significant difference from values for the no-treatment group and with a P value of <0.001 indicating a significant difference from values for the itaconic acid-only group] and 2.7 ± 0.51 for treatment with ceftazidime plus itaconic acid [with a P values of <0.001 indicating a significant difference from values for the no-treatment group and a with a P value <0.001 indicating a significant difference from values for the itaconic acid-only group]).

DISCUSSION

Our recent development of animal infection models for acute and chronic melioidosis has allowed us to address important questions concerning those factors that control the outcome of lung infection due to *B. pseudomallei* (36). We have determined that ICL, an enzyme of the glyoxylate shunt, is essential for the establishment of chronic *B. pseudomallei* infection (Table 1). Therefore, ICL is a persistence factor for *B. pseudomallei*. Although it is tempting to conclude that the ability to metabolize fatty acids is essential for the production of persistent *B. pseudomallei* infection, our results suggest that this is not the case. The mutation of ICL or other genes involved in the TCA cycle or fatty acid metabolism did not eliminate *B. pseudomallei* growth on C₂ or C₃ carbon sources (data not shown). Since *B. pseudomallei* has a very large metabolic potential, it is possible that single or double mutations in key metabolic pathways do not prevent growth on distinct carbon sources (34).

Although ICL is a persistence factor for both *B. pseudomallei* and *M. tuberculosis* (17, 21), in *B. pseudomallei*, in contrast with *M. tuberculosis*, this is not due to an inability to metabolize fatty acids. It could, however, be argued that even though ICL is a persistence factor for *M. tuberculosis*, fatty acid metabolism may not be the entire explanation. The mutation of ICL-1 in *M. tuberculosis* causes no effect during acute infection but eliminates the ability to cause a chronic infection (17). However, the *M. tuberculosis* ICL-1 mutant strain can still grow on acetate as the sole carbon source because it still has a functional ICL-2 enzyme, indicating that it can still metabolize fatty acids (21). Furthermore, ICL-1 and ICL-2 can also function as MCL in the methyl-citrate cycle, which is involved in the metabolism of odd-chain fatty acids (23). However, the mutation of other enzymes required for the methyl-citrate cycle does not reduce the ability of *M. tuberculosis* to survive in vivo (23). Furthermore, it was previously suggested that the attenuation of ICL-1/ICL-2-deficient strains of *M. tuberculosis* is not due to an inability to metabolize fatty acids but rather is due to the accumulation of toxic propionate metabolites (35).

As *B. pseudomallei* strains lacking essential enzymes of the glyoxylate shunt and methyl-citrate cycle can still grow on propionate, we cannot comment on the effects that the accumulation of toxic propionate metabolites may have on virulence; however, the lack of key enzymes from the glyoxylate shunt and the methyl-citrate cycle seems to force *B. pseudomallei* into an acute infectious phase. Therefore, it is possible that the ability to metabolize fatty acids has no correlation to the requirement of ICL for the establishment of a chronic infection. In addition, although the requirement of ICL may not be correlated with its ability to metabolize fatty acids, we cannot negate the fact that fatty acids are the likely source of carbon during chronic pulmonary infections (22).

Our results have shown that MCL can act as an ICL in the absence of ICL activity (Fig. 2C). These observations, combined with the increased virulence of the ICL mutant and the slight decrease in virulence of the MCL mutant, indicate that the enzymatic function of ICL is not its only function in persistence (Tables 1 and 2). We argue that this is also the case for *M. tuberculosis* because ICL-2 is functional in an ICL-1 mutant

strain (21). If it was solely the enzymatic function that was essential for persistence, the virulent phenotypes of the ICL and MCL mutants would be similar, as they both have parental ICL enzymatic activity (Fig. 2C). Again, for *M. tuberculosis*, both ICL-1 and ICL-2 mutant strains should have the same phenotype in vivo; however, it is only the ICL-1 mutant that is unable to establish a chronic infection (17, 21). In addition, it could also be concluded that the increase in ICL activity may contribute to the decreased virulence seen for the ACN strain and the increased ability to establish a persistent or chronic infection (Tables 1 and 2 and Fig. 2C). Alternatively, *B. pseudomallei* ACN could function as an enzyme in the TCA cycle and also as an iron-dependent RNA binding protein like ACN of *M. tuberculosis* (1). Therefore, the lack of the ACN iron-dependent RNA binding function would lead to the observed reduction in virulence, as there is no reduction in the enzymatic activity of the *B. pseudomallei* ACN mutant strain (Tables 1 and 2 and Fig. 2B).

The virulence of the *B. pseudomallei* parental and mutant strains was well correlated to their cytotoxicity toward macrophage cells (Fig. 3B to D). The ICL mutants were significantly more cytotoxic whereas the ACN mutant was significantly less cytotoxic than the parental DD503 strain (Fig. 3B to D). The differences in cytotoxicity were noted in the absence of differences in the abilities of the parental and mutant strains to survive within unactivated macrophage cells (Fig. 3A). Again, the increased cytotoxicity of these strains cannot be accounted for solely by a decrease in the level of ICL enzymatic activity because MCL can potentially substitute for ICL in the single mutants (Fig. 2C). However, the enzymatic activity of ICL does play a role in virulence, as the ICL-MCL double mutant that has reduced ICL enzymatic activity is hypervirulent. Therefore, ICL of *B. pseudomallei* may function like ICL of *M. tuberculosis* to increase intracellular survival (14). In addition, the increases in levels of cytotoxicity correlate well with the increased virulence of the *B. pseudomallei* ICL mutant strains (Tables 1 and 2). This suggests that the loss of ICL activity alerts the *B. pseudomallei* strains to activity kill the macrophage cells, resulting in a switch from a chronic to an acute infectious state.

Even though ICL is a persistence factor for both *B. pseudomallei* and *M. tuberculosis*, the mutation of this gene results in very different clinical outcomes during animal infections (17, 21). A mutation of ICL-1 in *M. tuberculosis* prevents the establishment of a chronic infection and results in a decrease in virulence (17). On the other hand, the mutation of ICL in *B. pseudomallei* prevents the establishment of a chronic infection and results in an increase in virulence (Tables 1 and 2). Therefore, forcing a chronic *M. tuberculosis* infection into an acute phase in an immunocompetent host results in the clearance of *M. tuberculosis*, and this is likely due to the slow doubling time and the potential accumulation of toxic propionate metabolites (17, 35). However, forcing a chronic *B. pseudomallei* infection into an acute phase in an immunocompetent host results in an overwhelming acute infection that significantly increases the morbidity and mortality of the host, and this is likely due to intrinsic virulence and the ability to metabolize propionate in the absence of ICL activity (Tables 1 and 2).

Therefore, caution should be used in the development of ICL inhibitors as novel antimicrobials because the inhibition of

ICL does not always result in a decrease in virulence. The inhibition of ICL activity during a chronic *B. pseudomallei* infection resulted in an overwhelming infection (Fig. 4C). This is significant, as previous results observed for chronic *B. pseudomallei* animal infections did not result in mortality even after 28 days of infection (36). Again, this supports the hypothesis that treatment with itaconic acid causes the nonreplicating bacteria to resume active growth, making them once again susceptible to antibiotic treatment. Indeed, we observed that treatment with itaconic acid plus ceftazidime reduced bacterial loads during chronic pulmonary *B. pseudomallei* infections more so than treatment with ceftazidime alone. These results have major implication for the development of ICL inhibitors as novel antimicrobials. Our results suggest that ICL inhibitors should not be developed solely as antimicrobials but could be used in combination with conventional antibiotics to treat not only *B. pseudomallei* infection but also *M. tuberculosis* infections.

ICL has also been implicated in the establishment of chronic infection by other bacteria including *Pseudomonas aeruginosa* (16) and *Salmonella enterica* serovar Typhimurium (7). One might take advantage of this common theme for persistent bacterial infections to determine whether itaconic acid could be used to “wake up” other dormant bacteria. For example, will this observation allow us to finally establish a link between *Mycobacterium paratuberculosis* and Crohn’s disease by “waking up” dormant bacteria (33)? In conclusion, it appears that itaconic acid treatment forces dormant bacteria into an actively replicating state, and the implications for the treatment of latent infections could be very exciting indeed.

ACKNOWLEDGMENTS

We are thankful to Herbert Schweizer for providing the mini-Tn7 constructs. We thank Laura Silo-Suh for helpful discussions and Jessica Hagins for advice on the enzymatic assays. We thank Paul Brett for information on the macrophage invasion assay. We thank Mark Gillrie for his assistance in taking the microscopic pathology images. We thank Richard Moore for critically reading the manuscript and Erica Wong for help with the figures.

The work was supported by CHIR operating grant MOP-36343, awarded to D.E.W., a Canada Research Chair in Microbiology.

REFERENCES

- Banerjee, S. A., K. Nandyala, P. Raviprasad, N. Ahmed, and S. E. Hasnain. 2007. Iron-dependent RNA-binding activity of *Mycobacterium tuberculosis* aconitase. *J. Bacteriol.* **189**:4046–4052.
- Burtneck, M. N., P. J. Brett, V. Nair, J. M. Warawa, D. E. Woods, and F. C. Gherardini. 2008. *Burkholderia pseudomallei* type III secretion system mutants exhibit delayed vacuolar escape phenotypes in RAW 264.7 murine macrophages. *Infect. Immun.* **76**:2991–3000.
- Choi, K. H., D. DeShazer, and H. P. Schweizer. 2006. Mini-Tn7 insertion in bacteria with multiple glmS-linked attTn7 sites: example *Burkholderia mallei* ATCC 23344. *Nat. Protoc.* **1**:162–169.
- Currie, B. J., D. A. Dance, and A. C. Cheng. 2008. The global distribution of *Burkholderia pseudomallei* and melioidosis: an update. *Trans. R. Soc. Trop. Med. Hyg.* **102**(Suppl. 1):1–4.
- Dance, D. A. B. 1991. Melioidosis: the tip of the iceberg? *Clin. Microbiol. Rev.* **4**:52–60.
- deLorenzo, V., and K. N. Timmis. 1994. Analysis and construction of stable phenotypes in gram-negative bacteria with Tn5- and Tn10-derived minitransposons. *Methods Enzymol.* **235**:386–405.
- Fang, F. C., S. J. Libby, M. E. Castor, and A. M. Fung. 2005. Isocitrate lyase (AceA) is required for *Salmonella* persistence but not for acute lethal infection in mice. *Infect. Immun.* **73**:2547–2549.
- Gan, Y. H. 2005. Interaction between *Burkholderia pseudomallei* and the host immune response: sleeping with the enemy? *J. Infect. Dis.* **192**:1845–1850.
- Gould, T. A., H. van de Langemheen, E. J. Muñoz-Eliás, J. D. McKinney, and J. C. Sacchettini. 2006. Dual role of isocitrate lyase 1 in the glyoxylate and methylcitrate cycles in *Mycobacterium tuberculosis*. *Mol. Microbiol.* **61**:940–947.
- Guy, E. S., and A. Mallampalli. 2008. Managing TB in the 21st century: existing and novel drug therapies. *Ther. Adv. Respir. Dis.* **2**:401–408.
- Heckman, K. L., and L. R. Pease. 2007. Gene splicing and mutagenesis by PCR-driven overlap extension. *Nat. Protoc.* **2**:924–932.
- Hiler, S., and W. T. Charnetzky. 1981. Glyoxylate bypass enzymes in *Yersinia* species and multiple forms of isocitrate lyase in *Yersinia pestis*. *J. Bacteriol.* **145**:452–458.
- Ip, M., G. Lars, P. Y. Osterberg, and T. Raffin. 1995. Pulmonary melioidosis. *Chest* **108**:1420–1424.
- Jun-Ming, L., L. Na, Z. Dao-Yin, W. La-Gen, H. Yong-Lin, and Y. Chun. 2008. Isocitrate lyase from *Mycobacterium tuberculosis* promotes survival of *Mycobacterium smegmatis* within macrophage by suppressing cell apoptosis. *Chin. Med. J.* **121**:1114–1119.
- Kanehisa, M., and S. Goto. 2000. KEGG: Kyoto encyclopedia of genes and genomes. *Nucleic Acids Res.* **28**:27–30.
- Lindsey, T. L., J. M. Hagins, P. A. Sokol, and L. A. Silo-Suh. 2008. Virulence determinants from a cystic fibrosis isolate of *Pseudomonas aeruginosa* include isocitrate lyase. *Microbiology* **154**:1616–1627.
- McKinney, J. D., K. Honer ze Bentrup, E. J. Muñoz-Eliás, A. Miczak, B. Chen, W. T. Chan, D. Swenson, J. C. Sacchettini, W. R. Jacobs, Jr., and D. G. Russell. 2000. Persistence of *Mycobacterium tuberculosis* in macrophages and mice requires the glyoxylate shunt enzyme isocitrate lyase. *Nature* **406**:735–738.
- Moore, R. A., D. DeShazer, S. Reckseidler, A. Weissman, and D. E. Woods. 1999. Efflux-mediated aminoglycoside and macrolide resistance in *Burkholderia pseudomallei*. *Antimicrob. Agents Chemother.* **43**:465–470.
- Moore, R. A., S. Reckseidler-Zenteno, H. Kim, W. Nierman, Y. Yu, A. Tuanyok, J. Warawa, D. DeShazer, and D. E. Woods. 2004. Contribution of gene loss to the pathogenic evolution of *Burkholderia pseudomallei* and *Burkholderia mallei*. *Infect. Immun.* **72**:4172–4187.
- Moore, R. A., A. Tuanyok, and D. E. Woods. 2008. Survival of *Burkholderia pseudomallei* in water. *BMC Res. Notes* **7**:1–11.
- Muñoz-Eliás, E. J., and J. D. McKinney. 2005. *Mycobacterium tuberculosis* isocitrate lyase 1 and 2 are jointly required for in vivo growth and virulence. *Nat. Med.* **11**:638–644.
- Muñoz-Eliás, E. J., and J. D. McKinney. 2006. Carbon metabolism of intracellular bacteria. *Cell. Microbiol.* **8**:10–22.
- Muñoz-Eliás, E. J., A. M. Upton, J. Cherian, and J. D. McKinney. 2006. Role of the methylcitrate cycle in *Mycobacterium tuberculosis* metabolism, intracellular growth, and virulence. *Mol. Microbiol.* **60**:1109–1122.
- My, L., and T. H. Ottenhoff. 2008. Not to wake a sleeping giant: new insights into host-pathogen interactions identify new targets for vaccination against latent *Mycobacterium tuberculosis* infection. *Biol. Chem.* **389**:497–511.
- Overtoom, R., V. Khieu, S. Hem, P. Cavailler, V. Te, S. Chan, P. Lau, B. Guillard, and S. Vong. 2008. A first report of pulmonary melioidosis in Cambodia. *Trans. R. Soc. Trop. Med. Hyg.* **102**(Suppl. 1):21–25.
- Peacock, S. J., H. P. Schweizer, D. A. Dance, T. L. Smith, J. E. Gee, V. Wuthiekanun, D. DeShazer, I. Steinmetz, P. Tan, and B. J. Currie. 2008. Management of accidental laboratory exposure to *Burkholderia pseudomallei* and *B. mallei*. *Emerg. Infect. Dis.* **14**:e2.
- Reckseidler-Zenteno, S., R. DeVinney, and D. E. Woods. 2005. The capsular polysaccharide of *Burkholderia pseudomallei* contributes to survival in serum by reducing complement factor C3b deposition. *Infect. Immun.* **73**:1106–1115.
- Reed, L. J., and H. Muench. 1938. A simple method of estimating fifty per cent endpoints. *Am. J. Hyg.* **27**:493–497.
- Schappinger, D., S. Ehrhart, M. I. Voskuil, Y. Liu, J. A. Mangan, I. M. Monahan, G. Dolganov, B. Efron, P. D. Butcher, C. Nathan, and G. K. Schoolnik. 2003. Transcriptional adaptation of *Mycobacterium tuberculosis* within macrophages: insight into the phagosomal environment. *J. Exp. Med.* **198**:693–704.
- Skorupski, K., and R. K. Taylor. 1996. Positive selection vectors for allelic exchange. *Gene* **169**:47–52.
- Somerville, G., C. A. Mikoryak, and L. Reitzer. 1999. Physiological characterization of *Pseudomonas aeruginosa* during exotoxin A synthesis: glutamate, iron limitation, and aconitase activity. *J. Bacteriol.* **181**:1072–1078.
- Somerville, G. A., B. Said-Salim, J. M. Wickman, S. J. Raffel, B. N. Kreiswirth, and J. M. Musser. 2003. Correlation of acetate catabolism and growth yield in *Staphylococcus aureus*: implications for host-pathogen interactions. *Infect. Immun.* **71**:4724–4732.
- Thomas, D. C. 2008. Cows, Crohn’s and more: is *Mycobacterium paratuberculosis* a superantigen? *Med. Hypotheses* **71**:838–861.
- Tuanyok, A., B. R. Leadem, R. K. Auerbach, S. M. Beckstrom-Sternberg, J. S. Beckstrom-Sternberg, M. Mayo, V. Wuthiekanun, T. S. Brettin, W. C. Nierman, S. J. Peacock, B. J. Currie, D. M. Wagner, and P. Keim. 2008. Genomic islands from five strains of *Burkholderia pseudomallei*. *BMC Genomics* **9**:566–583.

35. **Upton, A. M., and J. D. McKinney.** 2007. Role of the methylcitrate cycle in propionate metabolism and detoxification in *Mycobacterium smegmatis*. *Microbiology* **153**:3973–3982.
36. **van Schaik, E., M. Tom, R. DeVinney, and D. E. Woods.** 2008. Development of novel animal infection models for the study of acute and chronic *Burkholderia pseudomallei* pulmonary infections. *Microbes Infect.* **10**:1291–1299.
37. **Vidyalakshmi, K., M. Chakrapani, B. Shrikala, S. Damodar, S. Lipika, and S. Vishal.** 2008. Tuberculosis mimicked by melioidosis. *Int. J. Tuberc. Lung Dis.* **12**:1209–1215.
38. **Wayne, L. G., and L. G. Hayes.** 1996. An in vitro model for sequential study of shutdown of *Mycobacterium tuberculosis* through two stages of nonreplicating persistence. *Infect. Immun.* **64**:2062–2069.
39. **White, N. J.** 2003. Melioidosis. *Lancet* **361**:1715–1722.

Editor: S. R. Blanke